

RESEARCH ARTICLE

A comprehensive analysis of non-pharmaceutical interventions and vaccination on Ebolavirus disease outbreak: Stochastic modeling approach

Youngsuk Ko¹, Jacob Lee², Yubin Seo², Eunok Jung^{1*}

1 Department of Mathematics, Konkuk University, Seoul, Korea, **2** Division of Infectious Disease, Hallym University College of Medicine, Seoul, Korea

* junge@konkuk.ac.kr**OPEN ACCESS**

Citation: Ko Y, Lee J, Seo Y, Jung E (2024) A comprehensive analysis of non-pharmaceutical interventions and vaccination on Ebolavirus disease outbreak: Stochastic modeling approach. *PLoS Negl Trop Dis* 18(6): e0011955. <https://doi.org/10.1371/journal.pntd.0011955>

Editor: Aleksandra Inic-Kanada, Medical University of Vienna, AUSTRIA

Received: February 1, 2024

Accepted: May 16, 2024

Published: June 7, 2024

Copyright: © 2024 Ko et al. This is an open access article distributed under the terms of the [Creative Commons Attribution License](https://creativecommons.org/licenses/by/4.0/), which permits unrestricted use, distribution, and reproduction in any medium, provided the original author and source are credited.

Data Availability Statement: The data that support the findings of this study are available in Figshare at dx.doi.org/10.6084/m9.figshare.25867198. These data were derived from the following resources available in the public domain: <https://www.afro.who.int/countries/publications?country=879>. Data used in our study are aggregated from WHO situation reports. (available at <https://www.afro.who.int/countries/publications?country=879>).

Funding: This research was supported by the Government-wide R&D Fund Project for Infectious

Abstract

Ebolavirus disease (EVD) outbreaks have intermittently occurred since the first documented case in the 1970s. Due to its transmission characteristics, large outbreaks have not been observed outside Africa. However, within the continent, significant outbreaks have been attributed to factors such as endemic diseases with similar symptoms and inadequate medical infrastructure, which complicate timely diagnosis. In this study, we employed a stochastic modeling approach to analyze the spread of EVD during the early stages of an outbreak, with an emphasis on inherent risks. We developed a model that considers healthcare workers and unreported cases, and assessed the effect of non-pharmaceutical interventions (NPIs) using actual data. Our results indicate that the implementation of NPIs led to a decrease in the transmission rate and infectious period by 30% and 40% respectively, following the declaration of the outbreak. We also investigated the risks associated with delayed outbreak recognition. Our simulations suggest that, when accounting for NPIs and recognition delays, prompt detection could have resulted in a similar outbreak scale, with approximately 50% of the baseline NPIs effect. Finally, we discussed the potential effects of a vaccination strategy as a follow-up measure after the outbreak declaration. Our findings suggest that a vaccination strategy can reduce both the burden of NPIs and the scale of the outbreak.

Author summary

Our research employs a stochastic model to analyze the early-stage spread of Ebolavirus Disease. We incorporated factors such as healthcare workers and unreported cases, and utilized real data to evaluate the impact of non-pharmaceutical interventions on disease transmission. Our findings indicate that rapid outbreak recognition could effectively control disease spread with reduced efforts. For example, if outbreak recognition occurred just one day after the first death, the level of non-pharmaceutical intervention required would have been 45% less than the baseline scenario, causing the same outbreak scale. On

Disease Research (GFID), Republic of Korea (grant No. HG23C1629 to YK, JL, YS, and EJ). This paper is supported by the Korea National Research Foundation (NRF) grant funded by the Korean government (MEST) (NRF-2021M3E5E308120711 to YK, JL, YS, and EJ). EJ received funding from GFID and NRF. YK, JL, YS, and EJ were supported by GFID and NRF. YK received salary from GFID and NRF. The funders had no role in study design, data collection and analysis, decision to publish, or preparation of the manuscript.

Competing interests: The authors have declared that no competing interests exist.

the contrary, a one-week delay in outbreak recognition required 50% higher non-pharmaceutical interventions. Furthermore, we explored the potential implementation of a vaccination strategy following an outbreak declaration. The vaccine administration, similar to early outbreak recognition, could reduce the burden of non-pharmaceutical interventions. In the model simulation, if 20% of the considered population (100,000) were vaccinated within 50 days after outbreak recognition, the level of non-pharmaceutical intervention required could be reduced by 40%. Our results suggest that such a strategy could mitigate both the scale of the outbreak and the necessity for additional interventions.

Introduction

Ebolavirus Disease (EVD) was first identified in 1976 in Sudan and the Democratic Republic of Congo [1, 2]. The scale and impact of EVD outbreaks have evolved over time. The 2013–2016 West Africa epidemic was notably the most severe outbreak, resulting in over 11,000 deaths [3]. The most recent outbreak occurred in Uganda in 2022, with the first case identified on September 19, leading to an official outbreak declaration the following day. This outbreak lasted approximately four months, with 164 confirmed cases and 77 deaths [4]. The management and response to EVD outbreaks pose several challenges. For instance, cases may go unreported due to the initial symptoms being easily mistaken for other diseases, leading to transmission to healthcare workers (HCWs) during the early stages of an outbreak [5, 6]. This challenge is particularly prevalent in remote areas and regions with limited medical facilities [7].

As of January 2024, two vaccines have been approved by World Health Organization: Ervebo and Zabdeno/Mvabea [8]. Ervebo, a single-dose vaccine, is primarily used for emergency response and has demonstrated near 100% efficacy in preventing infection immediately after vaccination [9]. However, it is only effective against Zaire ebolavirus and has poor storage stability, requiring use within 4 hours at room temperature and temperatures below -60°C for long-term storage [10]. In contrast, Zabdeno/Mvabea, a two-dose vaccine administered to healthcare workers in advance, is speculated to have a relatively lesser preventive effect than Ervebo [10]. It requires an 8-week vaccination period for the two doses, making it unsuitable for immediate outbreak response, but it has better storage stability, remaining viable for up to a year while Ervebo lasts for 14 days at regular refrigerator temperatures ($+2$ to $+8^{\circ}\text{C}$) [10].

The application of these vaccines during outbreaks offers further insights. During the 2013–2016 West Africa outbreak, ring vaccination commenced in April 2015, a period when the outbreak was subsiding. The vaccination was experimental, with a small number of approximately 3,000 individuals vaccinated compared to the overall scale of the outbreak, and the effectiveness of the vaccine was measured during the same period [11]. In the 2018–2020 Kivu epidemic, vaccination started a week after the outbreak was declared, and approximately 300,000 individuals were vaccinated in total [12]. However, despite rapid recognition and the application of both non-pharmaceutical interventions (NPIs) and vaccination, controlling the spread was challenging due to conflict, insecurity, and misinformation [13–15].

NPIs are public health measures that aim to prevent or control the spread of infectious diseases without the use of pharmaceutical drugs [16]. While pharmaceutical interventions are crucial in the fight against EVD, their import and distribution processes can be time-consuming and complex [17]. Therefore, the role of NPIs becomes paramount, especially in the early stages of an outbreak or in regions where access to medical treatments is limited. These include personal preventive measures (such as personal protective equipment) and community

measures (such as contact tracing, social distancing, and travel restrictions), which reduce both of transmissibility and the contagious period.

Utilizing mathematical modeling to study infectious diseases provides a systematic structure that is crucial for deciphering and forecasting disease transmission dynamics [18, 19]. A significant advantage of such modeling is its ability to provide quantitative insights. Rather than making decisions based on general observations, these models utilize detailed numerical data. This precise data assists policymakers in understanding the outcomes of potential interventions, including vaccination campaigns, travel restrictions, and the enforcement of social distancing measures [20–22]. There are studies which have primarily focused on the mathematical modeling of transmission dynamics and control strategies related to EVD outbreaks. Previous research has investigated the initial transmission patterns during the 2014 West African EVD outbreak to quantify the disease's transmissibility and the impact of NPIs [23, 24]. The potential risks associated with importing the pathogen into non-African countries and the inherent threats of large-scale outbreaks were examined [25, 26]. Contact tracing have utilized strategies to assess the effectiveness of various containment and intervention approaches [27, 28].

There are studies which have concentrated on vaccination strategies for EVD outbreaks. Masterson analyzed the required level of preventive vaccines based on the basic reproduction number within a population and concluded that the ideal vaccination coverage is unrealistic due to the high requirement [29]. Chowell used an individual-based model to evaluate the impact of vaccine strategies on outbreak control and found that ring vaccination alone would not be effective in controlling the epidemic in situations where there is a delay in vaccination [30]. Wells conducted a spread analysis in Congo using a spatiotemporal model and observed that the vaccine program reduced the risk areas by up to 70.4% and decreased the risk level within those areas by up to 70.1% [31]. Potluri found that if preventive vaccine strategies are applied to HCWs and the general population, the scale and mortality of EVD outbreaks can be significantly reduced, even considering only imperfect vaccine effects [32]. Lastly, Bisanzio conducted an individual based modeling study which shows that preventive vaccination, including HCWs, frontline workers, and the general population, alongside NPIs, can significantly reduce Ebola cases and deaths, and flatten epidemic curves [33].

In this study, we investigated the early stages of the EVD outbreak, considering various key factors associated with potential risks. In modeling the EVD outbreak, we adopted a comprehensive approach by considering the roles of HCWs, unreported cases, and the lag between the emergence and detection of the initial case while assessing the effect of NPIs, including vaccination strategies. While some of the factors we incorporated for EVD have been investigated in previous research, our methodology is comprehensive, integrating various elements such as unreported cases, HCWs, NPIs, and vaccines into a single detailed model. This approach allows us to measure outcomes through scenario-based analysis, providing a thorough view of the situation.

Materials and methods

Modeling of EVD outbreak

In the modeling of the EVD outbreak, we considered the following groups: susceptible (S), exposed (before symptom onset, E), infectious (post-symptom onset, I), hospitalized (Q), and recovered (R). We further divided the infectious group into I_1 and I_2 to differentiate between reported and unreported cases. We incorporated homogeneous mixing disease transmission into our model, which does not differentiate between local spread and nosocomial infection. We hypothesized that hospitalized patients were effectively isolated and could not transmit the

disease. Note that we did not reflect the phenomenon that reported cases can die before hospitalization. Still, there is a possibility of immediate death upon hospitalization. We incorporated HCWs by adding groups with the subscript M , and assumed that there are no unreported cases among the HCWs. Fig 1 outlines the entire progression of the disease. Solid arrows indicate infection events characterized by non-delayed reactions (Markovian processes). In contrast, dashed arrows denote disease progression and delayed reactions, which are non-Markovian processes. Considering both of delayed and non-delayed reactions, our model can be formulated as delay differential equations:

$$\begin{aligned}
 \frac{dS}{dt} &= -\beta S \frac{I_1 + I_2 + I_M}{N}, \\
 \frac{dS_M}{dt} &= -p_M \beta S_M \frac{I_1 + I_2 + I_M}{N}, \\
 \frac{dE}{dt} &= \beta S \frac{I_1 + I_2 + I_M}{N} - E(t - \tau_{E \rightarrow I}), \\
 \frac{dE_M}{dt} &= p_M \beta S_M \frac{I_1 + I_2 + I_M}{N} - E_M(t - \tau_{E \rightarrow I}), \\
 \frac{dI_1}{dt} &= \rho E(t - \tau_{E \rightarrow I}) - I_1(t - \tau_{I_1 \rightarrow H}), \\
 \frac{dI_2}{dt} &= (1 - \rho) E(t - \tau_{E \rightarrow I}) - (1 - f) I_2(t - \tau_{I_2 \rightarrow R}) - f I_2(t - \tau'_{I_2 \rightarrow R}), \\
 \frac{dI_M}{dt} &= E_M(t - \tau_{E \rightarrow I}) - I_M(t - \tau_{I_M \rightarrow H}), \\
 \frac{dH}{dt} &= I_1(t - \tau_{I_1 \rightarrow H}) + I_M(t - \tau_{I_M \rightarrow H}) - (1 - f) H(t - \tau_{H \rightarrow R}) - f H(t - \tau'_{H \rightarrow R}), \\
 \frac{dR}{dt} &= (1 - f) (I_2(t - \tau_{I_2 \rightarrow R}) + H(t - \tau_{H \rightarrow R})),
 \end{aligned}
 \tag{1}$$

where $N = S + S_M + E + E_M + I_1 + I_2 + I_M + R$.

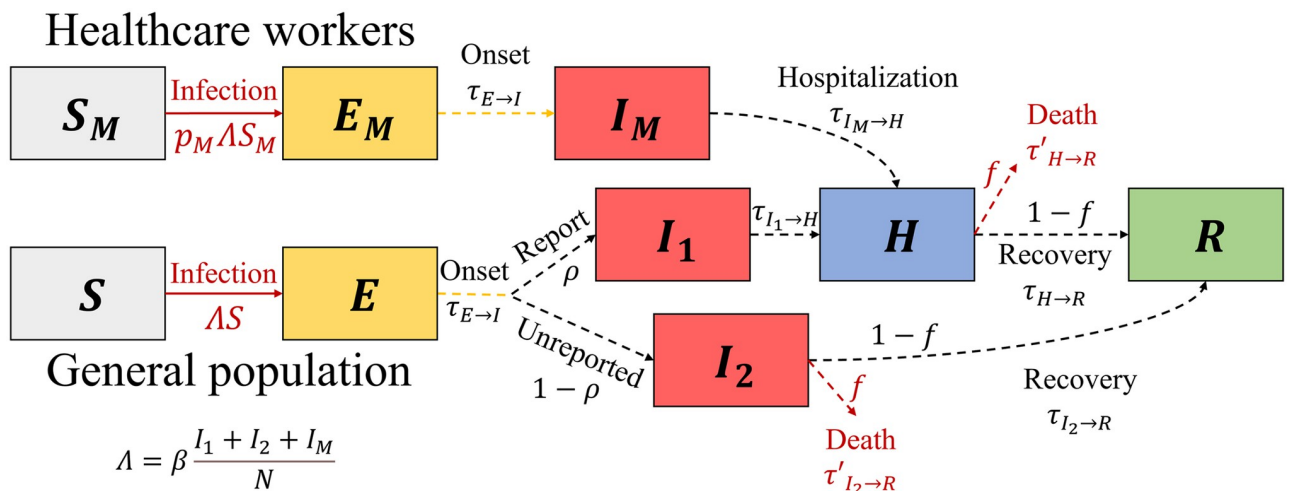


Fig 1. Flow diagram of the Ebolavirus disease transmission model. Healthcare workers and unreported cases are considered. Solid-line arrows signify nondelayed reactions, whereas dashed-line arrows denote delayed reactions.

<https://doi.org/10.1371/journal.pntd.0011955.g001>

Table 1. Characteristics of the propensity of nondelayed events and details of delayed events.

Event	Type	Description	Reference
Infection of HCWs	Nondelayed	Propensity: $p_M \beta S_M \frac{I_1 + I_2 + I_M}{N}$	[34–36]
Infection of non-HCWs	Nondelayed	Propensity: $\beta S \frac{I_1 + I_2 + I_M}{N}$	[34–36, 39, 40]
From exposure to onset ($\tau_{E \rightarrow I}$)	Delayed	Log-normal distribution, Mean: 9, SD: 4.31	[43–45]
Symptom onset to hospitalization (non-HCWs, $\tau_{I_1 \rightarrow Q}$)	Delayed	Uniform distribution, 5.79 ± 3.30	[35, 36]
Symptom onset to hospitalization (HCWs, $\tau_{I_M \rightarrow Q}$)	Delayed	Uniform distribution, 0.5 ± 0.5	Assumed, [41, 42]
From hospitalization to recovery ($\tau_{H \rightarrow R}$)	Delayed	Uniform distribution, 20.38 ± 7.58	[35, 36]
From hospitalization to death ($\tau'_{H \rightarrow R}$)	Delayed	Uniform distribution, $5.56 \pm 6.11^*$	[35, 36]

*If the generated value is lesser than 0, then the value changes to 0. In real, this is the case when the patient dies before the hospitalization.

<https://doi.org/10.1371/journal.pntd.0011955.t001>

The parameter β is the transmission rate and p_M represents the heightened risk factor associated with HCWs. To parameterize p_M , we used the case number ratio of non-HCWs to HCWs (50:14) and the population size ratio (1000:1.1) in Mubende province where the study was conducted. As a result, p_M is determined to be 254.55. These data indicated that HCWs poses a greater risk of infection by 254.55. We estimated the value of β without NPIs at 0.19, assuming that the basic reproductive number is 2.5 and the average infectious period is 5.79 days [34–36]. We set the case fatality rate f to 0.44 [37]. The subsequent subsection discusses the report rate, represented by ρ , which varies based on the outbreak detection. Time delays are applied using τ where subscripts indicate the transition, and be listed in Table 1.

We used modified Gillespie algorithm to simulate our model and ran 10,000 runs per scenario [38]. Table 1 offers a comprehensive breakdown of the propensities associated with non-delayed events and the particulars of delayed events, which are aggregated from past epidemiological investigations and described using time delay τ in Eq 1 [34–36, 39–45]. We assumed a uniform distribution of delays, except for the incubation period, owing to a lack of data. Note that we assumed lesser transmissibility of HCWs, due to their professional training and direct involvement in treating patients, by setting short infectious period [41, 42]. We set the infectious period of unreported cases to be identical to the duration of hospitalization for reported cases, taking into account their outcomes (either recovery or death), i.e., $\tau_{I_2 \rightarrow R} = \tau_{H \rightarrow R}$ and $\tau'_{I_2 \rightarrow R} = \tau'_{H \rightarrow R}$.

Scenarios for model simulation

For a baseline scenario, we focused on the outbreak within the Mubende district, the epicenter of the 2022 Ugandan EVD outbreak. The simulation encompassed two stages, accounting for behavioral alterations and NPIs after the outbreak announcement: the phase before the declaration (P1) and after the declaration (P2). Fig 2 graphically describes and clarifies this phase division. A primary case refers to an individual introducing the infection into a population, whereas an index case denotes the first identified case [46]. The primary case can be the index case, but not necessarily. We set that the primary case is non-HCW in the unreported infectious state (I_2), and the population size is 100,110 (100,000 non-HCWs and 110 HCWs) [40].

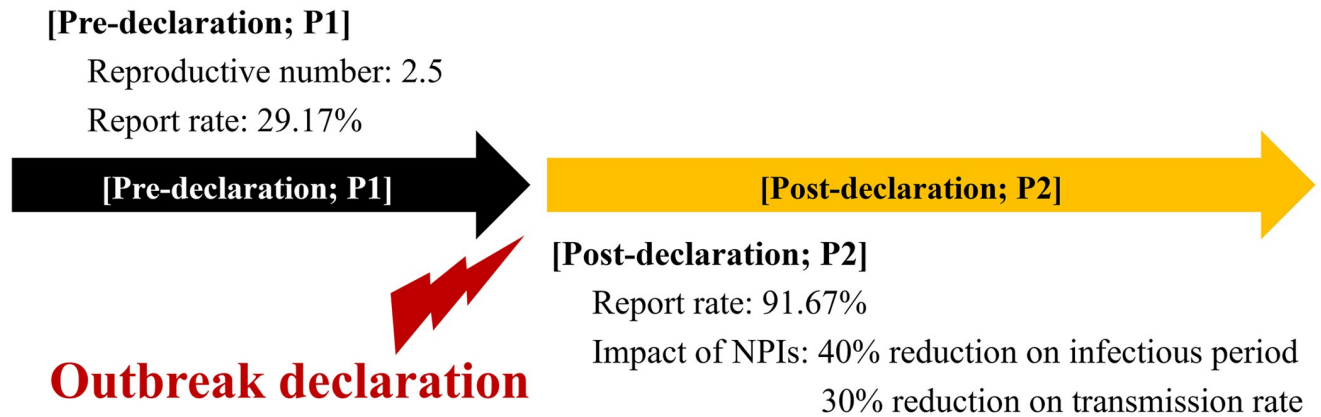


Fig 2. Division of phases considering outbreak declaration and setting for baseline model simulation scenario.

<https://doi.org/10.1371/journal.pntd.0011955.g002>

To set the effect of NPIs for the baseline scenario, we assumed that the transmission rate and duration from symptom onset to hospitalization decreased by 30% and 40%, respectively, upon outbreak declaration. Note that these coupled values are chosen, as the values would be most plausible among possible combinations, to simulate real incidence and described in subsequent section. The criterion for this declaration was 19 days after the first death, which is within the reported group and consistent with the situation in Uganda. In 2022, it was ascertained in Mubende district that six deaths, later confirmed, had occurred before the official outbreak declaration [47, 48]. Investigations indicated the potential for 17 more probable deaths before this declaration [49]. Based on these data, the reporting rate in the pre-declaration phase was estimated to be 7/24 (29.17%). In the post-declaration phase, with 22 confirmed deaths and two probable deaths, the estimated rate was 22/24 (91.67%). The report rate also shifted (from P_1 to P_2) when the outbreak was declared. Furthermore, based on the difference between the two reporting rates, we assumed that individuals in group I_2 transition to I_1 at the outbreak declaration and are reported later.

To consider comparable scenarios, we explored the effects of varying the thresholds for outbreak declaration, the intensity of NPIs on the spread of the disease, and vaccination. Note that there is no vaccination in the baseline scenario. In the scenario considering vaccination, it reflects vaccine availability or the effectiveness of the vaccine. A insufficient supply of vaccines (or low effectiveness) is explained by a low vaccination proportion and a long duration. Since there is no vaccine against Sudan ebolavirus, we assumed hypothetical vaccine which has similar effectiveness as Ervebo. The key variations considered are as follows:

- **Threshold for outbreak declaration:** The delay from the first death to outbreak declaration varied from 1 to 38 days.
- **Effect of NPIs:** The effect of NPIs on the transmission rate and infectious period varied. This variation ranged from a 50% reduction (more stringent NPIs) to an increase of 50% (less severe NPIs) relative to the baseline setting.
- **Vaccination:** To simply reflect the duration of vaccination and the time it takes to become immune after vaccination, we assume that once a certain time has passed, vaccinated hosts become immune. That is, hosts in state S transfer to R once the vaccination duration (minimum 20 days, maximum 80 days) has passed after the outbreak declaration. The proportion of vaccinated individuals ranges from 0.1 to 0.3, while all HCWs are vaccinated.

Results

Baseline scenario simulation

Fig 3 shows the baseline simulation results for cumulative confirmed cases. The gray curves depict the outcomes of each distinct simulation run, the dark curve signifies the mean, and the red boxes show the trends of confirmed cases in Mubende district. Because of inherent randomness, the timing of the outbreak declaration differs across runs; therefore, all simulation outcomes were synchronized based on the timing of the outbreak declaration. The actual number of confirmed cases in Mubende District was 66. The simulation mean value was 66.84 (95% credible interval (CrI): 0-226).

In the baseline scenario simulation, the transmission rate and duration from symptom onset to hospitalization (infection period) were reduced by 30% and 40%, respectively, following the outbreak declaration. Thus, the real-world effect of NPIs closely mirrors these levels. Nevertheless, the decline in the transmission rate might have been more pronounced, whereas the reduction in the duration from symptom onset to hospitalization might have been less significant or the inverse. Fig 4A shows the contour lines for pairs of values with an average closely aligned with the actual data, spanning a range of the effect of NPIs. Red asterisk indicates values for the baseline scenario (40% and 30% of reduction of infectious period and transmissibility, respectively). When comparing the X- and Y-axis intercepts, scenarios with no reduction in the infectious period but a 70% reduction in the transmission rate and those with no decrease in the transmission rate but a 53% reduction in the infectious period showed similar simulation results. Fig 4B shows the outbreak duration from the simulation runs when NPIs follow the contour line in Fig 4A. When the impact of NPIs on the infectious period is at its maximum (53%) or minimum (0%), the mean outbreak becomes 94 (95% CrI: 14-163) or 120 (95% CrI: 16-238), respectively.

Fig 5A presents the distribution of duration from primary case to outbreak declaration (P_1), which reveals a bimodal pattern. Outbreaks are typically declared within seven days, with

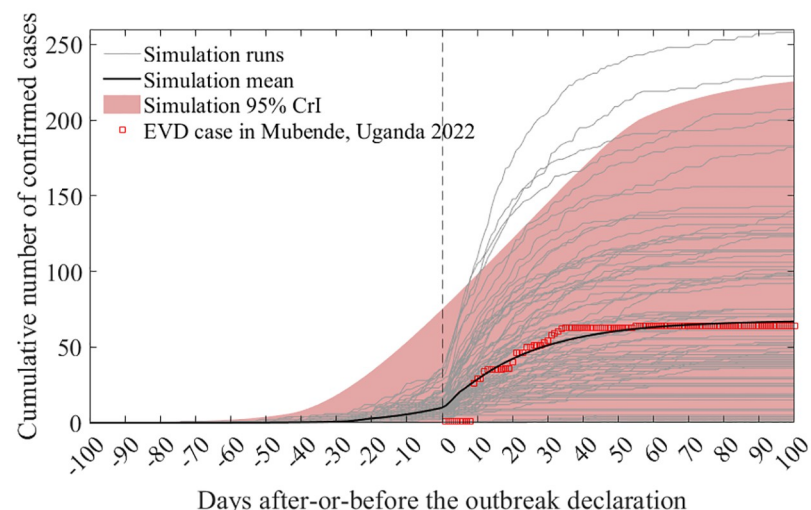


Fig 3. Cumulative confirmed cases from the baseline model simulation. The grey curves represent individual simulation runs, the dark curve denotes the simulation mean, and the red boxes display actual data from the Mubende district. Note that the vertical line, marking time 0, signifies the timing of the outbreak declaration in the simulation runs.

<https://doi.org/10.1371/journal.pntd.0011955.g003>

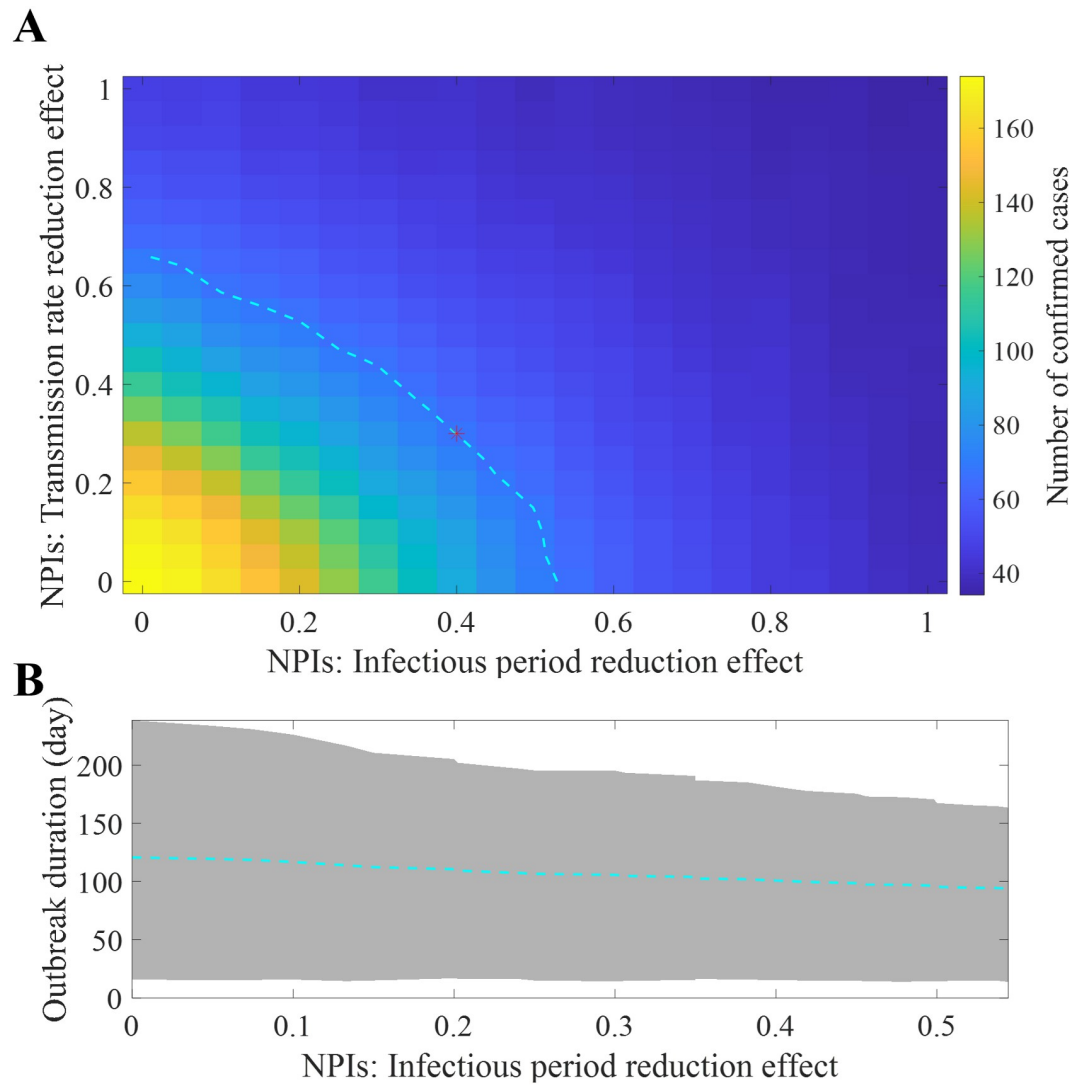


Fig 4. Effect of NPIs on the simulation results. Impact of NPIs on confirmed cases, where the dashed cyan curve represents the contour line with an mean value equivalent to the baseline scenario simulation outcome. (A), mean and 95% CrI of the outbreak duration over of contour line in A (B).

<https://doi.org/10.1371/journal.pntd.0011955.g004>

another cluster emerging at approximately 50 days. This distinct pattern arises in some simulation scenarios where subsequent infections do not manifest, leading to the premature end of the outbreak. The probability of an outbreak concluding prematurely within one week was 19%, which indicates the case where the disease dies out before the declaration. On average, excluding instances where the disease ended early, the primary case manifested approximately 50 days prior (95% CrI: 32-82). Fig 5B shows the distribution of P2 duration and exhibits a monomodal distribution, with a mean of 64 days (95% CrI: 9-147). In this study, we defined the duration of P2 as the period from outbreak declaration to when there were no individuals in stages E or I.

Addressing how many individuals were infected when the outbreak declaration was officially acknowledged is essential for planning and responding. Fig 6 illustrates the distribution of prevalence by status at the outbreak declaration. Mean number (95% CrI) of E, E_M, I₁, I₂, and I_M are 12.07, 3.04, 1.64, 7.34, and 0.16 (0-45, 0-11, 0-7, 0-27, and 0-1), respectively. When

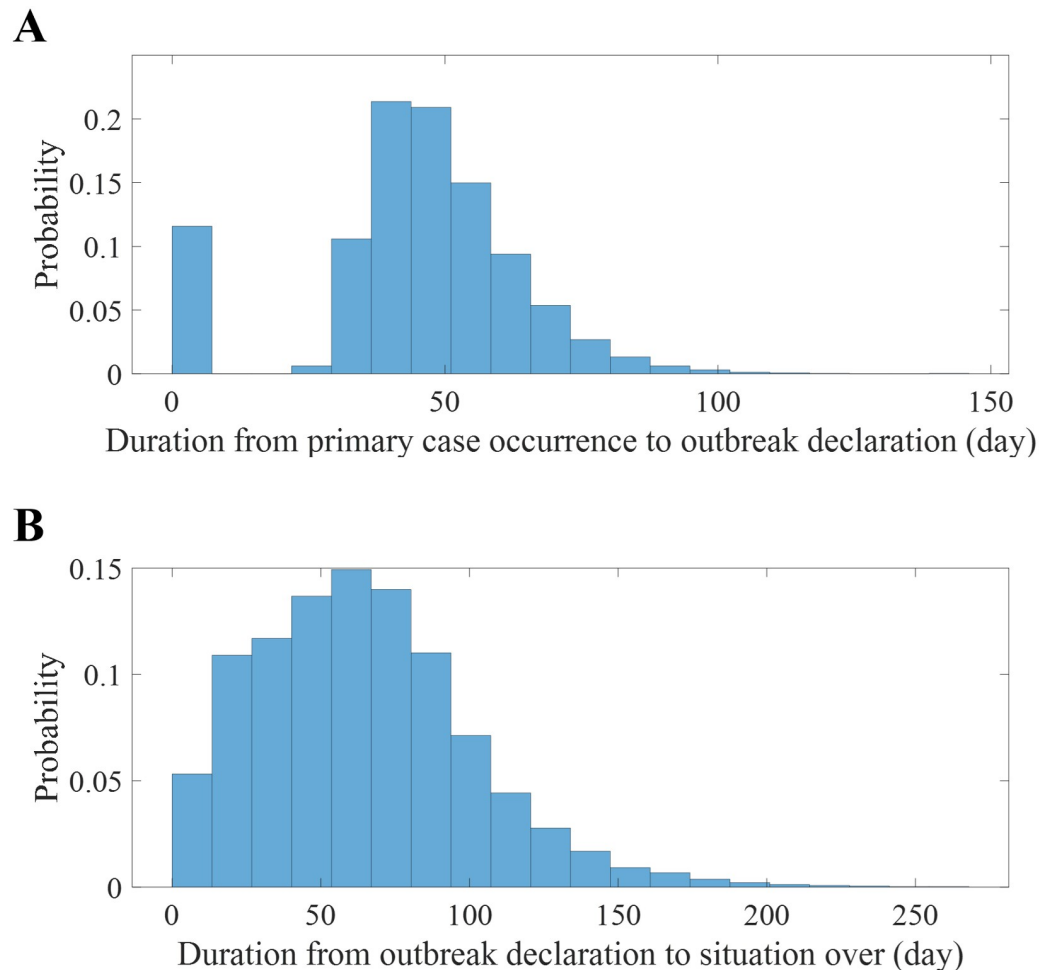


Fig 5. Histogram representing the durations of phases. Duration from the occurrence of the primary case to the outbreak declaration (A), and from the outbreak declaration to the end of outbreak (B).

<https://doi.org/10.1371/journal.pntd.0011955.g005>

normalized by population size, the number of exposed HCWs is 27.62 per 1,000. This ratio is 229 times higher than the non-HCWs group, which registers at 0.12 per 1,000.

Sensitivity analysis for the baseline scenario

Sensitivity analysis is a powerful tool used in mathematical modeling and simulation studies [50]. It allows us to understand how different input parameters influence the output of a model. By varying the inputs within a certain range, we can observe how the output changes, thereby identifying which inputs have the most significant impact on the model results. To conduct the sensitivity analysis, we calculated the Partial Rank Correlation Coefficient (PRCC) [50]. We examined four parameters as model inputs: the effect of NPIs on both transmission rate and infectious period, the duration from the first death to the outbreak declaration, the transmission rate, and the report rate before the outbreak declaration. We set uniform distributions ranging $\pm 50\%$ based on the baseline scenario for these parameters, and set 200,000 parameter combinations for Latin Hypercube Sampling. The number of infections (transition from susceptible to exposed) was set as the model output. Fig 7 displays the value of PRCC

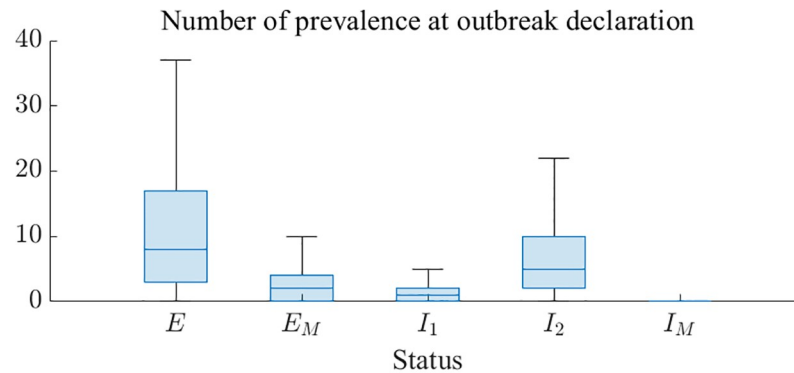


Fig 6. Distribution of infected individuals at the time of outbreak declaration.

<https://doi.org/10.1371/journal.pntd.0011955.g006>

over time: Fig 7A shows the PRCC for each input, and Fig 7B shows the absolute PRCC values changing over time. Note that we considered dummy input (dashed line in Fig 7B) to test the robustness of the model, and the maximum absolute value of PRCC was lesser than 0.003. The ranges of PRCC for the effect of NPIs on both transmission rate and infectious period, the duration from the first death to the outbreak declaration, the transmission rate, and the report rate before the outbreak declaration were measured as $[-0.17, 0.00]$, $[0.14, 0.34]$, $[0.11, 0.64]$, and $[-0.10, -0.08]$, respectively. The report rate showed the smallest change in PRCC. The input that had the most significant impact in the past has shifted from declaration delay to transmission rate. The effect of NPIs on the transmission rate and the infectious period was 0 before the outbreak declaration and gradually increased afterwards, becoming more significant than both declaration delay and report rate.

Scenarios considering NPIs and outbreak detection

We conducted an examination of the distribution of confirmed case numbers under a variety of conditions. These conditions ranged from a span of 1 to 38 days between the first death and the declaration of the outbreak. Additionally, we considered variations in the NPIs level, which ranged from -50% to +50% relative to the baseline scenario. Fig 8A (Fig 8B) shows the delay range (NPIs levels) on the x-axis against the number of confirmed cases on the y-axis. As expected, with an increase in the delay, the number of infections also increased, exhibiting an exponential rather than a linear growth pattern. Within the 95% CrI, the maximum outbreak size surged from 111 individuals when declared a day after the first death to 523 after a 38-day delay. On the other hand, the number of cases decreases as NPIs level increases, 43 in the minimum (95% CrI: 0-161) once NPIs level is maximized. When the NPIs level is set as minimum (-50%), the mean number of cases reaches 177 (95% CrI: 0-585).

Here, we present the outcomes of simulations that concurrently adjust for the previously discussed factors: the timing of outbreak recognition and the intensity of NPIs. Fig 9 maps the NPI intensity on the x-axis against the duration from the first death occurrence to the outbreak declaration on the y-axis. The mean number of cases in each simulation setting is depicted using a color map. For comparison with the baseline scenario outcomes, we integrated contour curves corresponding to the average number of infections in the baseline scenario (white, 67) and half (green) and double (red) that count into the graph.

After examining the baseline contour, if an outbreak is declared merely a day after the first death, the intensity of the NPIs can be diminished by 45% to attain a similar outbreak

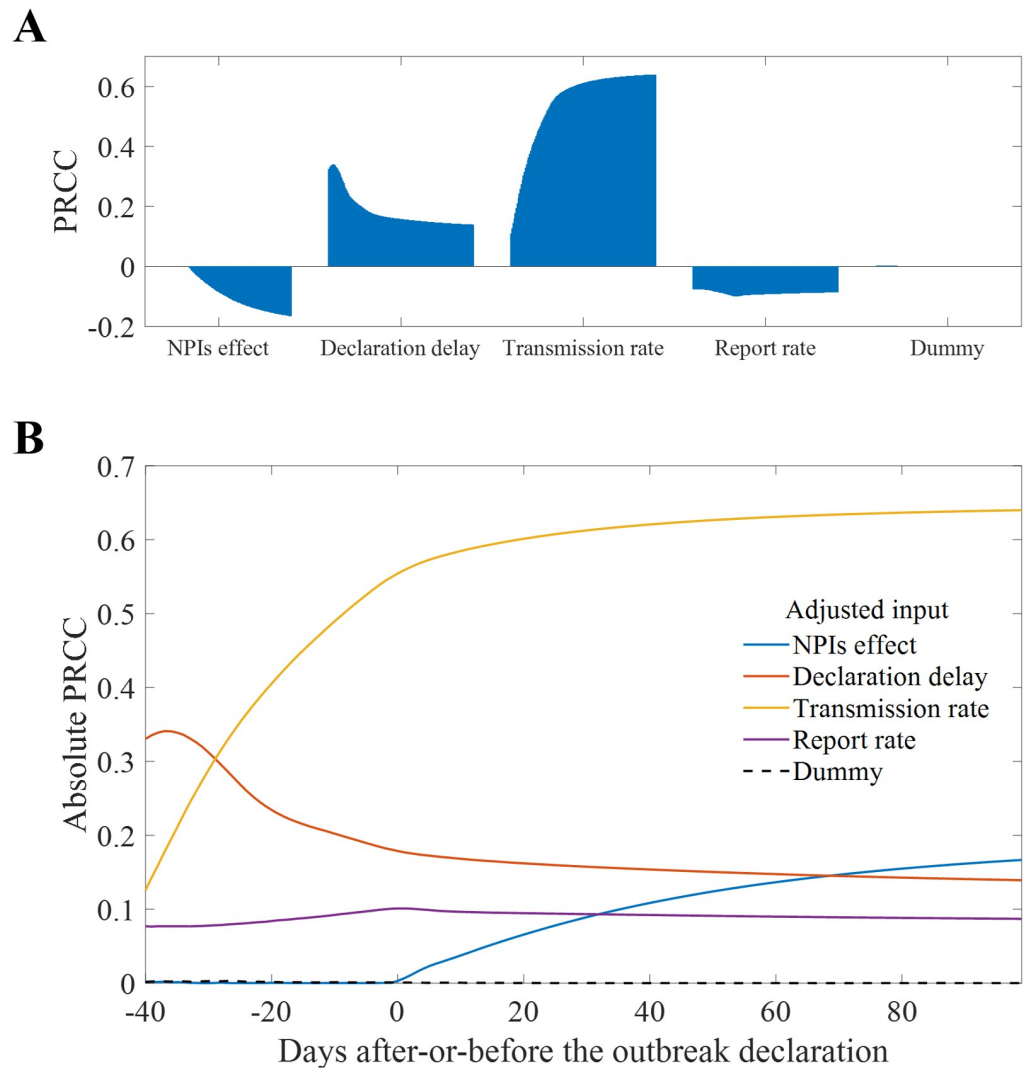


Fig 7. Parameter sensitivity analysis results. Time dependent PRCC by parameters (A), Absolute value of PRCC over time (B).

<https://doi.org/10.1371/journal.pntd.0011955.g007>

magnitude. By contrast, if the outbreak declaration occurs 26 days after the first death, the NPIs must be augmented by 50% to match the baseline outbreak scale. Given a constant NPIs level, outbreak recognition must be advanced by approximately two weeks to cut the infection count by half. Conversely, even with increased NPIs at the baseline recognition juncture, halving the infection scale was impossible.

Scenarios considering vaccination

Let us examine the effect of the vaccination strategy. Fig 10 depicts the mean number of confirmed cases in relation to the timing of when the vaccination is completed. The color of the curves (blue, red, and yellow) represents the proportion of the population that has been vaccinated (10, 20, and 30%). As the vaccination process is expedited or a larger proportion of the population is vaccinated, the number of cases decreases. Conversely, if the vaccination is delayed, the number of cases converges to the number in the baseline scenario (approximately

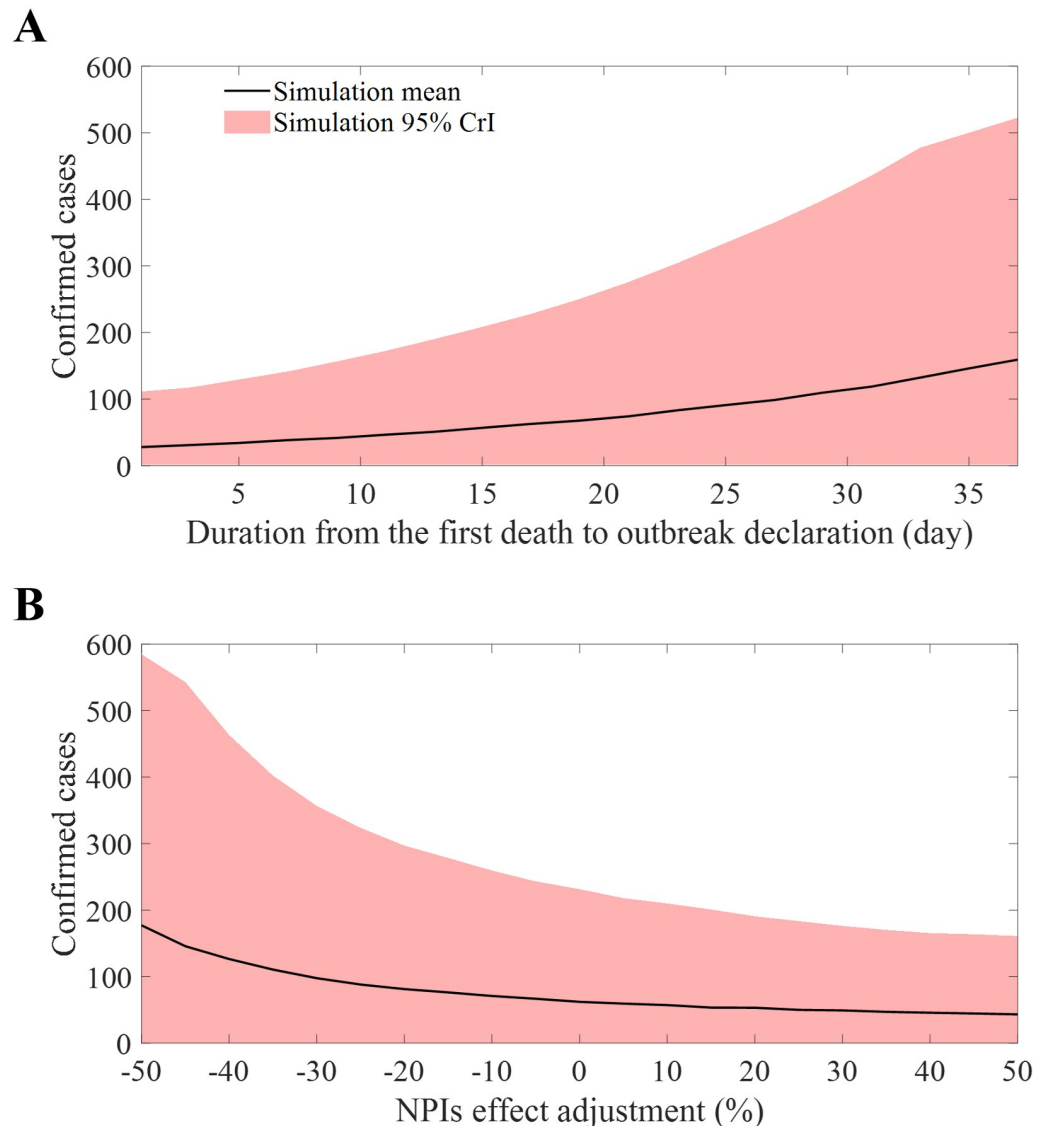


Fig 8. Mean and 95% CrI of confirmed cases considering different factors. Periods leading to outbreak declaration (A), relative intensity of NPIs (B).

<https://doi.org/10.1371/journal.pntd.0011955.g008>

67). Additionally, we verified whether there were significant changes in the simulation results indicated in Fig 10 as the vaccination period changed, using the Wilcoxon signed-rank test. We conducted a verification to see if the distribution of simulation runs varied depending on the vaccination duration for each vaccination proportion, and the Wilcoxon signed-rank test was applied to a total of 63 combinations. As a result of the verification, when the vaccination proportion was 10%, there was no significant difference when the vaccination duration was 60 days or more. When the vaccination proportion was 20%, there was no significant difference between the cases of 60 and 70 days. When the vaccination proportion reached 30%, there was always a significant difference when the vaccination duration was different. Table 2 lists simulation results. Note that the duration from primary case occurrence to outbreak declaration (P_1) was not considered in this table, because NPIs and vaccines are post-outbreak measures.

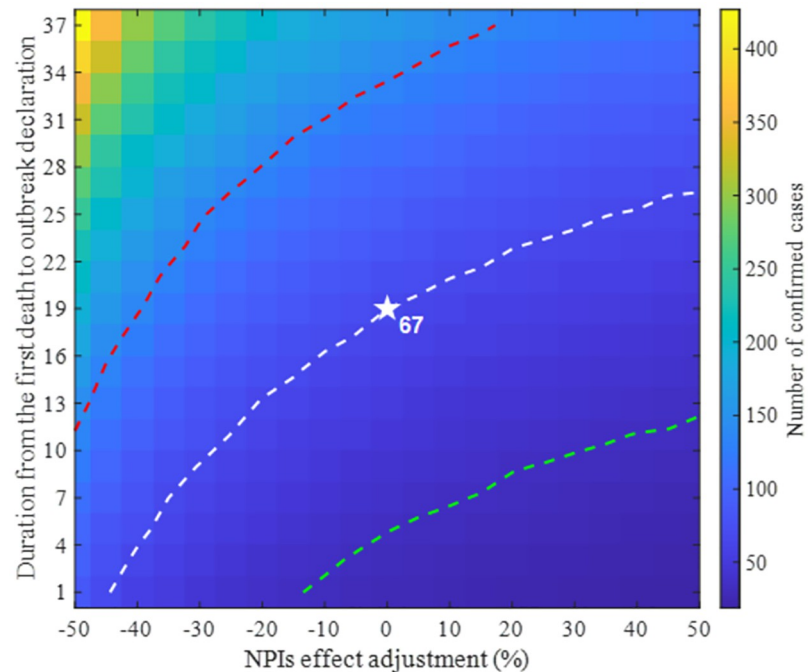


Fig 9. Outbreak scale determined by the intensity of NPIs and the timing of outbreak recognition. Dashed curves represent contours: white denotes the outbreak scale from the baseline, whereas green and red indicate half and double the size of the baseline simulation, respectively.

<https://doi.org/10.1371/journal.pntd.0011955.g009>

Similar to what Fig 9 represents, Fig 11 displays mean number of confirmed cases considering vaccination timing and the intensity of NPIs simultaneously. Fig 11A to 11C contain different simulation results considering various vaccinated proportion of individuals. Fig 11D displays contour curves aggregated from results in Fig 11A to 11C. Solid (dashed) curves indicate the mean (half mean) number of confirmed cases from the baseline scenario. If the vaccination proportion is set to be 20% and is finalized 50 days after the outbreak declaration, the intensity of NPIs that result in the same number of infections as the baseline scenario was

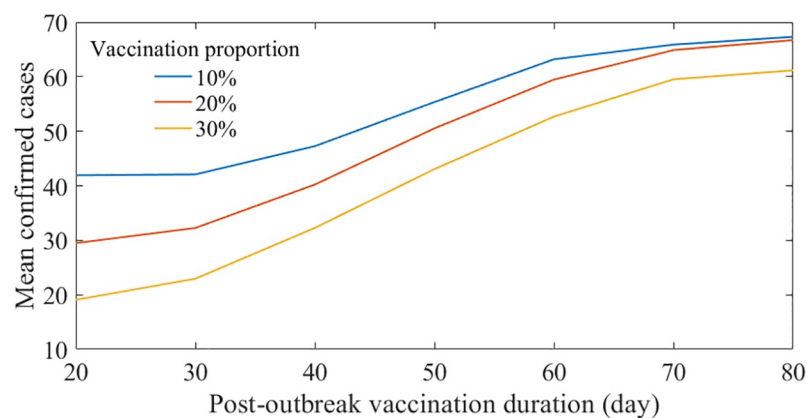


Fig 10. Mean number of confirmed cases considering vaccination strategy. X- and y- axis indicate the duration from outbreak declaration to the vaccination finalizing time and mean number of confirmed cases, respectively.

<https://doi.org/10.1371/journal.pntd.0011955.g010>

Table 2. Simulation results considering different vaccination rate and duration after outbreak declaration.

vaccination rate	ddd	Confirmed cases		Outbreak duration (P2)	
		mean	95% CrI	mean	95% CrI
10	20	42	[1, 157]	99	[15, 194]
	30	42	[1, 150]	98	[15, 192]
	40	47	[1, 154]	99	[15, 182]
	50	55	[1, 177]	103	[16, 186]
	60	63	[1, 214]	105	[15, 185]
	70	66	[1, 222]	107	[16, 193]
	80	67	[1, 236]	108	[15, 191]
20	20	29	[1, 108]	89	[14, 178]
	30	32	[1, 107]	89	[14, 173]
	40	40	[1, 123]	94	[14, 170]
	50	51	[1, 162]	98	[14, 171]
	60	59	[1, 193]	103	[15, 176]
	70	65	[1, 221]	106	[15, 182]
	80	67	[1, 231]	107	[14, 189]
30	20	19	[0, 69]	75	[7, 159]
	30	23	[0, 76]	76	[7, 153]
	40	32	[0, 101]	82	[7, 151]
	50	43	[0, 145]	88	[7, 159]
	60	53	[0, 190]	93	[7, 165]
	70	60	[0, 215]	97	[7, 172]
	80	61	[0, 225]	98	[7, 183]

<https://doi.org/10.1371/journal.pntd.0011955.t002>

reduced by 40%. Intersection of the blue solid curve and yellow dashed curve indicates the scenario where the confirmed cases could be reduced by half if vaccines can be administered three folds in the same 35 days with 40% eased NPIs.

Discussion

Our study introduces an investigation of EVD outbreak in Mubende province of Uganda, from the occurrence of the primary case to the detection of the index case and the end of the local outbreak, using a stochastic model. Instead of a national-scale outbreak, we observed the course of an outbreak that could occur in a single community and the associated detection delays. This allowed us to demonstrate the potential risk of spread to surrounding areas and the effectiveness of vaccination interventions (which could be considered a broad-scale ring vaccination) for smaller areas, in conjunction with NPIs.

Our model structure, which distinguishes between HCWs and non-HCWs as well as reported and unreported cases, provides a detailed understanding of the transmission dynamics. A simple observation of the data reveals a high risk of HCWs exposure, given the proportion of HCWs to the total population and the number of infected individuals. This underscores the need for enhanced protective measures and training [6]. As Fig 6 indicates, numerous HCWs could be exposed to the disease, necessitating early and aggressive interventions to identify cases targeting HCWs. Our model shows that an outbreak outcome can be highly uncertain. This is because it starts with a primary case and the disease progression, including the infectious period, can vary significantly. As results, our simulations show that the number of confirmed cases could range from 0 to 266 in 95% CrI. In the event of an actual

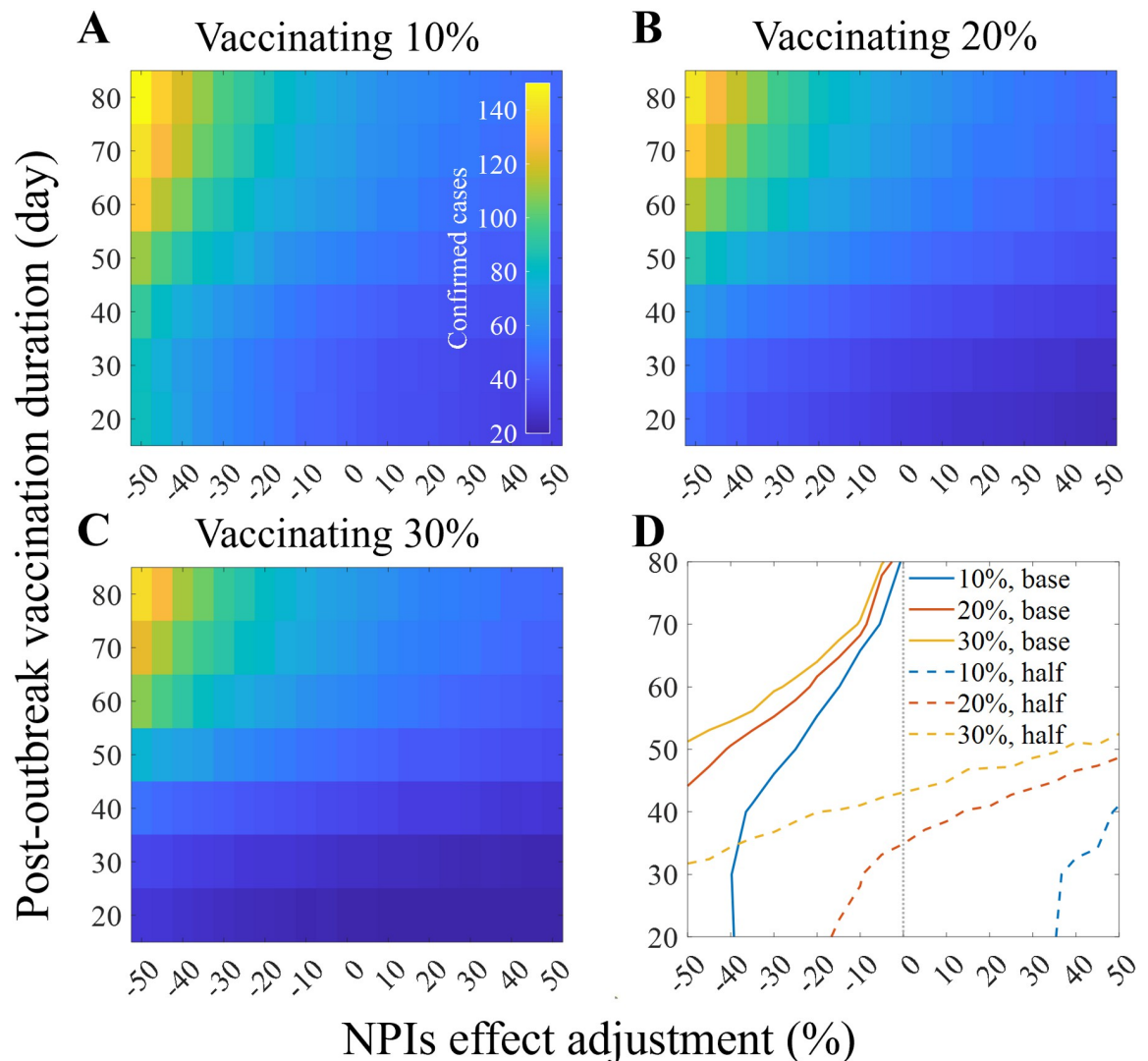


Fig 11. Impact of NPIs and vaccination application. Mean number of confirmed cases where 10%, 20%, 30% of individuals are vaccinated (A-C), contour lines representing the mean number of confirmed cases occurred in the baseline scenario (solid) and half of it (dashed) where the vertical dashed grey line indicates the baseline NPIs intensity (D).

<https://doi.org/10.1371/journal.pntd.0011955.g011>

outbreak, symptomatic infections can be distinguished. However, without precise testing, it is challenging to know how many individuals are in the incubation period. Fig 6 is expected to be able to present the level of risk that frontline workers should consider by showing how many individuals are actually in the incubation state. The sensitivity analysis of parameters, as depicted in Fig 7, further elucidates the key parameters that significantly influence the scale of the outbreak. While the results were intuitively perceived, they emphasized the factors influencing the situation quantitatively. The high sensitivity of the declaration delay (maximum PRCC: 0.34) just before the outbreak emphasized the importance of early detection. The sensitivity of the effect of NPIs (minimum PRCC: -0.17), which continues to increase after the outbreak declaration, emphasized the importance of interventions to reduce infections after the outbreak is recognized.

The simulation based on the baseline scenario indicates the potential range of real-world effects that NPIs could have on reducing both the transmission rate and the infectious period. The simulation of the baseline scenario suggests that the real-world impact of NPIs closely reflects the reduction in the transmission rate and the duration from symptom onset to hospitalization. Furthermore, our simulation results proposed a variety of NPIs that could have been implemented in real-world scenarios.

For example, we estimated the effects of NPIs on the transmission rate and infectious period to be 30% and 40%, respectively. However, as Fig 4 demonstrates, these could have been a combination of different values. This result also suggests the need for estimating the infectious period through epidemiological investigations. If a reduction in the infectious period due to NPIs can be estimated, then the effect of reducing the transmission rate could be measured immediately. Our simulation results show the potential to decrease the scale of an outbreak by shortening the infectious period or reducing the transmission rate.

The patterns observed in past EVD outbreaks are evident: late detection, inadequate intervention, misinformation, and larger, interconnected populations exacerbate the situation. The West Africa and Kivu epidemics, two significant EVD outbreaks, were the result of these factors. Our model simulation, which did not account for nationwide populations, could not predict an epidemic of that magnitude. However, our simulation still demonstrated exponential growth in the number of confirmed cases as detection was delayed (Fig 8A). On the other hand, in regions with low inter-regional connectivity and population density, small-scale outbreaks could occur even with misdiagnosis/diagnostic delays, as evidenced by the Gabon outbreak in 1994 [51].

Our scenario-based study, which varied the timing of the outbreak declaration and the intensity of NPIs (Fig 9), provides valuable insights for policymakers. In the two extreme cases, when an outbreak is detected a day after the first death, the same outbreak scale as the baseline scenario was observed even if the intensity of NPIs decreased by 45%. On the other hand, if there is a 7-day extra delay in detection compared to the baseline scenario, a 50% stronger intervention intensity needs to be applied to achieve the same outbreak scale. The results suggest that early recognition and declaration of an outbreak can significantly mitigate the intensity of NPIs required to control the outbreak similarly. In contrast, delays in outbreak recognition necessitate more aggressive NPIs to control outbreak. Localized interventions aimed at identifying confirmed cases among patients with EVD-like symptoms are less burdensome in terms of cost, effort, and human resource requirements than regional lockdowns and nationwide interventions. These findings underscore the importance of early detection.

Vaccine intervention has been observed to significantly reduce the outbreak size, duration, and the burden of NPIs. However, given the storage characteristics of vaccines and the state of medical infrastructure, it is inevitable that the introduction of vaccines will take time. This paradoxically emphasizes the importance of NPIs (Fig 11). If the targeted scale of the outbreak is similar, even if the same amount of vaccination is planned, a stronger intervention may be needed if it is delayed. As shown in Fig 11D, the scale of the outbreak can vary depending on the intervention environment (NPIs or vaccination). The simulation demonstrated the need to consider all these factors simultaneously for appropriate control below the risk level. As the reactive vaccination strategy we demonstrated was highly effective, the effects of proactive vaccination would be even stronger as previous studies showed [29–31]. In other words, if we can reflect the risk areas, we may see the highest vaccine effects shown in the past studies. Moreover, even with rapid vaccination, there may be limitations to the vaccine supply. As observed during the Kivu epidemic, when rapid vaccination was implemented, NPIs remained necessary and effective measures. The simulation was conducted based on the Everbo vaccine, which is highly effective with a single dose. However, the Everbo vaccine is effective against the

Zaire ebolavirus, and the case in Uganda involved the Sudan ebolavirus, not the Zaire ebolavirus. This highlights the need for vaccine development, as simulations have shown that the burden of NPIs in future outbreak situations would decrease if a vaccine is available.

This study had several limitations. Firstly, although the HCWs group was considered separately in the population, the locations where they stay (hospitals or clinics) were not distinguished. Because of the assumption of homogeneous mixing, the model could not consider close contact transmission routes such as households that can become places of infection outside of hospitals. Additionally, the vaccination did not reflect the target age of the vaccine. For instance, in the case of Eberbo, the target age was 17 years and older, but this study did not reflect the target age and only used a certain percentage of the total population [52]. Furthermore, the risk of transmission due to the EVD-transmissible semen of recovered patients, found in several cases during past EVD outbreaks, was not reflected [53]. Since we considered a model considering homogeneous mixing in a small community, our model could not simulate ring vaccination corresponding to individual contact networks. These limitations will be investigated using individual-based models in future work.

Author Contributions

Conceptualization: Youngsuk Ko, Jacob Lee, Eunok Jung.

Data curation: Youngsuk Ko.

Formal analysis: Youngsuk Ko, Jacob Lee, Yubin Seo.

Funding acquisition: Eunok Jung.

Investigation: Youngsuk Ko, Jacob Lee, Eunok Jung.

Methodology: Youngsuk Ko, Yubin Seo.

Project administration: Eunok Jung.

Resources: Youngsuk Ko.

Software: Youngsuk Ko.

Supervision: Yubin Seo, Eunok Jung.

Validation: Youngsuk Ko, Yubin Seo.

Visualization: Youngsuk Ko.

Writing – original draft: Youngsuk Ko, Eunok Jung.

Writing – review & editing: Youngsuk Ko, Eunok Jung.

References

1. Report of a WHO/International Study Team. Ebola haemorrhagic fever in Sudan, 1976. *Bulletin of the World Health Organization*. 1978; 56(2):247.
2. Report of an International Commission. Ebola haemorrhagic fever in Zaire, 1976. *Bulletin of the World Health Organization*. 1978; 56(2):271–93.
3. World Health Organization. Ebola outbreak 2014–2016—West Africa [Internet]. [cited 2024 Jan 12]. Available from: <https://www.who.int/emergencies/situations/ebola-outbreak-2014-2016-West-Africa>
4. World Health Organization. Ebola Disease caused by Sudan virus—Uganda [Internet]. 2022 [cited 2024 Jan 12]. Available from: <https://www.who.int/emergencies/disease-outbreak-news/item/2022-DON410>
5. Okeke IN. *Divining without seeds: the case for strengthening laboratory medicine in Africa*. Cornell University Press; 2011.

6. Suwantarant N, Apisarnthanarak A. Risks to healthcare workers with emerging diseases: lessons from MERS-CoV, Ebola, SARS, and avian flu. *Current opinion in infectious diseases*. 2015; 28(4):349–61. <https://doi.org/10.1097/QCO.000000000000183> PMID: 26098498
7. Scarpino SV, Iamarino A, Wells C, Yamin D, Ndeffo-Mbah M, Wenzel NS, et al. Epidemiological and viral genomic sequence analysis of the 2014 Ebola outbreak reveals clustered transmission. *Clinical Infectious Diseases*. 2015 Apr 1; 60(7):1079–82. <https://doi.org/10.1093/cid/ciu1131> PMID: 25516185
8. World Health Organization. Ebola virus disease: Vaccines [Internet]. 2020 [cited 2024 Jan 12]. Available from: <https://www.who.int/news-room/questions-and-answers/item/ebola-vaccines>
9. Henao-Restrepo AM, Camacho A, Longini IM, Watson CH, Edmunds WJ, Egger M, et al. Efficacy and effectiveness of an rVSV-vectored vaccine in preventing Ebola virus disease: final results from the Guinea ring vaccination, open-label, cluster-randomised trial (Ebola Ça Suffit!). *The Lancet*. 2017 Feb 4; 389(10068):505–18. [https://doi.org/10.1016/S0140-6736\(16\)32621-6](https://doi.org/10.1016/S0140-6736(16)32621-6) PMID: 28017403
10. Woolsey C, Geisbert TW. Current state of Ebola virus vaccines: A snapshot. *PLoS pathogens*. 2021 Dec 9; 17(12):e1010078. <https://doi.org/10.1371/journal.ppat.1010078> PMID: 34882741
11. Henao-Restrepo AM, Longini IM, Egger M, Dean NE, Edmunds WJ, Camacho A, et al. Efficacy and effectiveness of an rVSV-vectored vaccine expressing Ebola surface glycoprotein: interim results from the Guinea ring vaccination cluster-randomised trial. *The Lancet*. 2015 Aug 29; 386(9996):857–66. [https://doi.org/10.1016/S0140-6736\(15\)61117-5](https://doi.org/10.1016/S0140-6736(15)61117-5) PMID: 26248676
12. World Health Organization. Ebola virus disease Democratic Republic of Congo: external situation report 98/ 2020 [Internet]. 2020 [Cited 2024 Jan 12]. Available from: <https://www.who.int/publications/i/item/10665-332654>
13. Masumbuko Claude K, Underschultz J, Hawkes MT. Social resistance drives persistent transmission of Ebola virus disease in Eastern Democratic Republic of Congo: a mixed-methods study. *PLoS One*. 2019 Sep 26; 14(9):e0223104. <https://doi.org/10.1371/journal.pone.0223104> PMID: 31557243
14. Vinck P, Pham PN, Bindu KK, Bedford J, Nilles EJ. Institutional trust and misinformation in the response to the 2018–19 Ebola outbreak in North Kivu, DR Congo: a population-based survey. *The Lancet Infectious Diseases*. 2019 May 1; 19(5):529–36. [https://doi.org/10.1016/S1473-3099\(19\)30063-5](https://doi.org/10.1016/S1473-3099(19)30063-5) PMID: 30928435
15. Spinney L. In Congo, fighting a virus and a groundswell of fake news. *Science*. 2019 Jan; 363(6424):213–4. <https://doi.org/10.1126/science.363.6424.213> PMID: 30655420
16. World Health Organization. Ebola virus disease- Fact sheets [Internet]. 2023 [Cited 2024 May 10]. Available from: <https://www.who.int/news-room/fact-sheets/detail/ebola-virus-disease>
17. Polonsky JA, Bhatia S, Fraser K, Hamlet A, Skarp J, Stopard IJ, et al. Feasibility, acceptability, and effectiveness of non-pharmaceutical interventions against infectious diseases among crisis-affected populations: a scoping review. *Infectious diseases of poverty*. 2022 Feb 10; 11(01):8–26. <https://doi.org/10.1186/s40249-022-00935-7> PMID: 35090570
18. Wormser GP, Pourbohloul B. *Modeling Infectious Diseases in Humans and Animals* By Matthew James Keeling and Pejman Rohani Princeton, NJ: Princeton University Press, 2008.
19. Shearer FM, Moss R, McVernon J, Ross JV, McCaw JM. Infectious disease pandemic planning and response: Incorporating decision analysis. *PLoS medicine*. 2020 Jan 9; 17(1):e1003018. <https://doi.org/10.1371/journal.pmed.1003018> PMID: 31917786
20. Panovska-Griffiths J. Can mathematical modelling solve the current Covid-19 crisis?. *BMC Public Health*. 2020 Dec; 20(1):1–3. <https://doi.org/10.1186/s12889-020-08671-z> PMID: 32331516
21. Science News. A mathematical model to help optimize vaccine development [Internet]. 2021 [Cited 2024 Jan 12]. Available from: <https://www.sciencedaily.com/releases/2021/10/211027134956.htm>
22. Wei Y, Sha F, Zhao Y, Jiang Q, Hao Y, Chen F. Better modelling of infectious diseases: lessons from covid-19 in China. *bmj*. 2021 Dec 2; 375. <https://doi.org/10.1136/bmj.n2365> PMID: 34852999
23. Nishiura H, Chowell G. Early transmission dynamics of Ebola virus disease (EVD), West Africa, March to August 2014. *Eurosurveillance*. 2014 Sep 11; 19(36):20894. <https://doi.org/10.2807/1560-7917.ES2014.19.36.20894> PMID: 25232919
24. Chretien JP, Riley S, George DB. Mathematical modeling of the West Africa Ebola epidemic. *Elife*. 2015 Dec 8; 4:e09186. <https://doi.org/10.7554/eLife.09186> PMID: 26646185
25. Chen T, K Leung R, Liu R, Chen F, Zhang X, Zhao J, Chen S. Risk of imported Ebola virus disease in China. *Travel medicine and infectious disease*. 2014 Nov 1; 12(6):650–8. <https://doi.org/10.1016/j.tmaid.2014.10.015> PMID: 25467086
26. Ko Y, Lee SM, Kim S, Ki M, Jung E. Ebola virus disease outbreak in Korea: use of a mathematical model and stochastic simulation to estimate risk. *Epidemiology and Health*. 2019; 41. <https://doi.org/10.4178/epih.e2019048> PMID: 31801320

27. Lekone PE, Finkenstädt BF. Statistical inference in a stochastic epidemic SEIR model with control intervention: Ebola as a case study. *Biometrics*. 2006 Dec; 62(4):1170–7. <https://doi.org/10.1111/j.1541-0420.2006.00609.x> PMID: 17156292
28. Chowell G, Nishiura H. Characterizing the transmission dynamics and control of ebola virus disease. *PLoS biology*. 2015 Jan 21; 13(1):e1002057. <https://doi.org/10.1371/journal.pbio.1002057> PMID: 25607595
29. Masterson SG, Lobel L, Carroll MW, Wass MN, Michaelis M. Herd immunity to ebolaviruses is not a realistic target for current vaccination strategies. *Frontiers in immunology*. 2018 May 9; 9:1025. <https://doi.org/10.3389/fimmu.2018.01025> PMID: 29867992
30. Chowell G, Tariq A, Kiskowski M. Vaccination strategies to control Ebola epidemics in the context of variable household inaccessibility levels. *PLOS Neglected Tropical Diseases*. 2019 Nov 21; 13(11):e0007814. <https://doi.org/10.1371/journal.pntd.0007814> PMID: 31751337
31. Wells CR, Pandey A, Parpia AS, Fitzpatrick MC, Meyers LA, Singer BH, Galvani AP. Ebola vaccination in the Democratic Republic of the Congo. *Proceedings of the National Academy of Sciences*. 2019 May 14; 116(20):10178–83. <https://doi.org/10.1073/pnas.1817329116>
32. Potluri R, Kumar A, Maheshwari V, Smith C, Oriol Mathieu V, Luhn K, et al. Impact of prophylactic vaccination strategies on Ebola virus transmission: a modeling analysis. *Plos one*. 2020 Apr 27; 15(4):e0230406. <https://doi.org/10.1371/journal.pone.0230406> PMID: 32339195
33. Bisanzio D, Davis AE, Talbird SE, Van Effelterre T, Metz L, Gaudig M, et al. Targeted preventive vaccination campaigns to reduce Ebola outbreaks: An individual-based modeling study. *Vaccine*. 2023 Jan 16; 41(3):684–93. <https://doi.org/10.1016/j.vaccine.2022.11.036> PMID: 36526505
34. Althaus CL. Estimating the reproduction number of Ebola virus (EBOV) during the 2014 outbreak in West Africa. *PLoS currents*. 2014 Sep 2; 6. <https://doi.org/10.1371/currents.outbreaks.91afb5e0f279e7f29e7056095255b288> PMID: 25642364
35. Qin E, Bi J, Zhao M, Wang Y, Guo T, Yan T, et al. Clinical features of patients with Ebola virus disease in Sierra Leone. *Clinical infectious diseases*. 2015 Aug 15; 61(4):491–5. <https://doi.org/10.1093/cid/civ319> PMID: 25995207
36. Ji YJ, Duan XZ, Gao XD, Li L, Li C, Ji D, et al. Clinical presentations and outcomes of patients with Ebola virus disease in Freetown, Sierra Leone. *Infectious diseases of poverty*. 2016 Dec; 5(1):1–0. <https://doi.org/10.1186/s40249-016-0195-9> PMID: 27806732
37. Ministry of Health, Republic of Uganda. Ebolavirus Disease Situation Report 49 [Internet]. 2022 [Cited 2024 Jan 12]. Available from: https://www.afro.who.int/sites/default/files/2022-11/Ug_EVD_SitRep%2349.pdf
38. Anderson DF. A modified next reaction method for simulating chemical systems with time dependent propensities and delays. *The Journal of chemical physics*. 2007 Dec 7; 127(21). <https://doi.org/10.1063/1.2799998> PMID: 18067349
39. Brinkhoff T. Uganda: Cities, Towns & Urban Localities. City Population; c2023 [Internet]. 2020 [Cited 2024 Jan 12]. Available from: <https://www.citypopulation.de/en/uganda/cities/>
40. Wemos, ACHEST. Uganda's human resources for health: paradoxes and dilemmas [Internet]. 2019 [Cited 2024 Jan 12]. Available from: https://www.wemos.org/wp-content/uploads/2023/03/Advocacy-brief-Ugandas-human-resources-for-health_paradoxes-and-dilemmas-2019.pdf
41. Mercy Corps. Chapter 5: Ebola's effect on healthcare systems in Africa [Internet]. 2019 [cited 2024 Apr 1]. Available from: <https://www.mercycorps.org/blog/ebola-outbreaks-africa-guide/chapter-5>
42. Mohamud AK, Ali IA, Ali AI, Dirie NI, Inchon P, Ahmed OA, Mohamud AA. Assessment of healthcare workers' knowledge and attitude on Ebola virus disease in Somalia: a multicenter nationwide survey. *BMC Public Health*. 2023 Aug 28; 23(1):1650. <https://doi.org/10.1186/s12889-023-16562-2> PMID: 37641041
43. Eichner M, Dowell SF, Firese N. Incubation period of Ebola hemorrhagic virus subtype Zaire. *Osong public health and research perspectives*. 2011 Jun 1; 2(1):3–7. <https://doi.org/10.1016/j.phrp.2011.04.001> PMID: 24159443
44. Van Kerkhove MD, Bento AI, Mills HL, Ferguson NM, Donnelly CA. A review of epidemiological parameters from Ebola outbreaks to inform early public health decision-making. *Scientific data*. 2015 May 26; 2(1):1–0. <https://doi.org/10.1038/sdata.2015.19> PMID: 26029377
45. Centers for Disease Control and Prevention. Ebola Disease: Signs and Symptoms [Internet]. 2023 [cited 2024 Apr 1]. Available from: <https://www.cdc.gov/vhf/ebola/symptoms/index.html>
46. Rothman KJ, Greenland S, Lash TL. *Modern epidemiology*. Philadelphia: Wolters Kluwer Health/Lippincott Williams & Wilkins; 2008.
47. World Health Organization. EBOLA VIRUS DISEASE OUTBREAK RESPONSE ACCOUNTABILITY FORUM—10 January 2023 [Internet]. 2023 [Cited 2024 Jan 12]. Available from: <https://www.afro.who>

[int/sites/default/files/2023-01/EBOLA%20VIRUS%20DISEASE%20OUTBREAK%20RESPONSE%20ACCOUNTABILITY%20FORUM%20-%2010%20January%202023.pdf](https://www.afro.who.int/sites/default/files/2023-01/EBOLA%20VIRUS%20DISEASE%20OUTBREAK%20RESPONSE%20ACCOUNTABILITY%20FORUM%20-%2010%20January%202023.pdf)

48. Ministry of Health, Government of Uganda. Uganda national response plan for Ebolavirus disease outbreak [Internet]. 2022 [cited 2024 Jan 12]. Available from: https://www.afro.who.int/sites/default/files/2022-11/National%20Sudan%20Ebolavirus%20Response%20Plan_UGA_07102022.pdf
49. Ministry of Health, Government of Uganda. Ebolavirus Disease Situation Report 10 [Internet]. 2022 [cited 2024 Jan 12]. Available from: <https://reliefweb.int/report/uganda/uganda-ebola-virus-disease-situation-report-no-10>
50. Marino S, Hogue IB, Ray CJ, Kirschner DE. A methodology for performing global uncertainty and sensitivity analysis in systems biology. *Journal of theoretical biology*. 2008 Sep 7; 254(1):178–96. <https://doi.org/10.1016/j.jtbi.2008.04.011> PMID: 18572196
51. Georges AJ, Leroy EM, Renaut AA, Benissan CT, Nabias RJ, Ngoc MT, et al. Ebola hemorrhagic fever outbreaks in Gabon, 1994–1997: epidemiologic and health control issues. *The Journal of infectious diseases*. 1999 Feb 1; 179:S65–75. <https://doi.org/10.1086/514290> PMID: 9988167
52. The United States Food and Drug Administration. FDA NEWS RELEASE, FDA Roundup: July 28, 2023 [Internet]. 2023 [cited 2024 Jan 12]. Available from: <https://www.fda.gov/news-events/press-announcements/fda-roundup-july-28-2023>
53. Sun J, Uwishema O, Kassem H, Abbass M, Uweis L, Rai A, et al. Ebola virus outbreak returns to the Democratic Republic of Congo: an urgent rising concern. *Annals of medicine and surgery*. 2022 Jul 1; 79:103958. <https://doi.org/10.1016/j.amsu.2022.103958> PMID: 35757313